Curvature effect on surface diffusion: The nanotube

D. J. Shu
Institute of Solid State Physics, Chinese Academia Sinica, 230031-Hefei, China

X. G. Gong
Department of Physics, Fudan University, Shanghai 200433, People's Republic of China
and Institute of Solid State Physics, Academia Sinica, 230031-Hefei, People's Republic of China

(Received 9 November 2000; accepted 2 April 2001)

Using an empirical Tersoff–Brenner many-body potential for the carbon atoms and a model Lennard-Jones interaction between the adatom and carbon atoms, the diffusion of an adatom over curved surfaces of C nanotubes is studied by calculating the potential energy surface and performing molecular dynamics simulation. The average curvature of the surface is found to have an important influence on the diffusion of the adatom. Positive curvature increases the diffusion barrier and corrugates the potential energy surface, while the negative curvature smoothes the potential energy surface, therefore it lowers the diffusion barrier. We also find that nanotube helicity can play an important role on the diffusion path, thus the adatom has different diffusion path for the armchair and zig–zag nanotube. The nature of the curvature effect on the surface diffusion is connected with the strain effect. © *2001 American Institute of Physics.* [DOI: 10.1063/1.1373644]

I. INTRODUCTION

Adatom diffusion plays a fundamental role in the microscopic mechanism of many surface processes,[1] such as adsorption and desorption, surface reaction, and crystal growth. In order to understand surface processes on the atomic scale, one must study how the adatom diffuses on the specific surface and how it is affected, for instance, by surfactants,[2–4] defects,[5] and the strain effect.[6] The strain effect has long been recognized as a critical factor in many surface processes such as the epitaxial growth.[7–10] It has been shown that the strain and its *sign* are very important for the diffusion on metal and semiconductor surfaces.[11–14] Within a certain range, tensile strain can increase the diffusion barrier, while the compressive strain usually smoothes the potential surface and makes the adatom diffuse more easily. Meanwhile the strain-relief defects have been used as templates for the confined nucleation of nanostructures from adatoms.[15] Most studies of adatom diffusion to date have focussed on flat or weakly vicinal surfaces, with little attention being paid to significantly deformed surfaces. As a matter of fact, diffusion on the deformed surface is of importance in many aspects involving molecular sieves,[16] such as, separations and catalysis.

A curved surface has properties which differ from those of a flat, strain-free surface because of bond deformation. This can be expected to lead to adatom diffusion processes different from those of an adatom on a flat surface. The discovery of the nanotube[17] opens the possibility of quantum sieves[18] and chemistry in nanotubes (for a review, see Ref. 19); adatom diffusion is obviously of fundamental importance in such systems. Recently, nanotubes have shown potential of hydrogen storage,[20] but the physics and chemistry of H_2 uptake and desorption in nanotubes are not well understood. Since adsorption and desorption processes are closely related to mass transport in nanotubes, study of adatom diffusion might shed light on why and how nanotubes can store significant amounts of hydrogen while graphite cannot.

In this paper, we investigate the diffusion pathways and the energy barriers for an adatom on the surfaces of carbon SWNTs with different helicities, and show, for the first time, the influence of the surface curvature on the adatom diffusion. We find that the diffusion barrier and diffusion paths are strongly curvature-dependent. For a flat graphite sheet with zero average curvature, an adatom is stable at the binding site [A, the hollow site in the hexagons, see Fig. 2(a)]. An adatom can migrate from the binding site A to its adjacent ones across the six bridge sites. When the graphite plane is bent along some axis into a nanotube,[21] the hexagonal symmetry is broken, and some favorable diffusion channels will be set up. In the case of armchair and zig–zag helicity as we will show below, there are two possible different pathways, namely, via ABA and via ACA, which are equivalent in the noncurved graphite plane.

The rest of the paper is organized as follows: in Sec. II, we are going to briefly describe the calculation details. The main results and discussions will be given in Sec. III, and finally a short summary will be presented in Sec. IV.

II. CALCULATION DETAILS

The interaction of the C atoms is described by an empirical Tersoff–Brenner many-body potential,[22]

$$E_b = \sum_i \sum_{j>i} [V_R(r_{ij}) - \overline{B}_{ij} V_A(r_{ij})], \tag{1}$$

where $\overline{B}_{ij}$ is a normalized bond order, $V_R(r_{ij})$ and $V_A(r_{ij})$ are the repulsive and attractive pair terms. This potential has been extensively used to model the carbon nanotube and to study their mechanical properties.[23] The graphite surface is found to be chemically inert for many kinds of adsorbed

 © 2001 American Institute of Physics

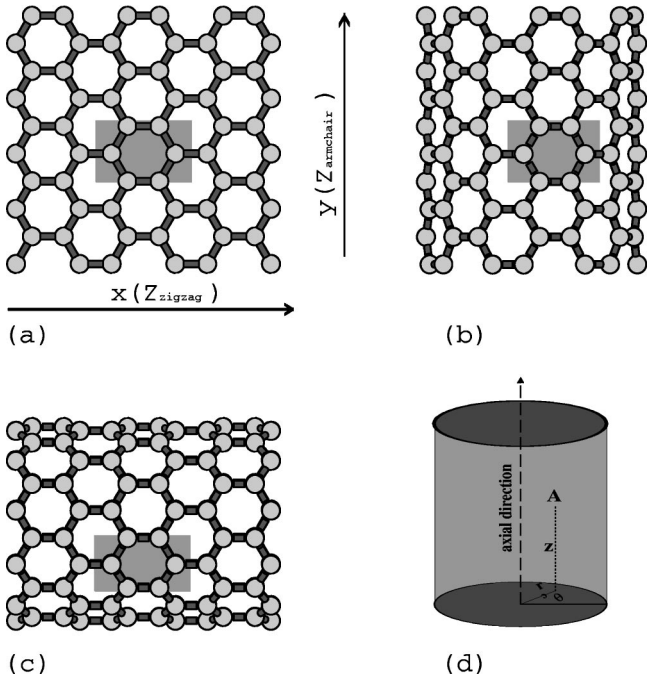

FIG. 1. Schematic display of the studied surfaces: (a) graphite plane; (b) zig–zag nanotube; (c) armchair nanotube; (d) is the frame of the cylindrical coordinate used to map an adatom in the nanotube. The shaded areas indicate the calculating unit cell.

atoms or molecules,[24,20] thus we use the Lennard-Jones potential (LJ) to model the interaction between the adatom and C atoms,[25–27]

$$V(r)=4\epsilon\left[\left(\frac{\sigma}{r}\right)^{12}-\left(\frac{\sigma}{r}\right)^{6}\right], \tag{2}$$

where two parameters σ and ϵ describe the radius and the strength of the interaction between the adatom and the C atoms. Since σ for the C atom is 3.4 Å, while σ for many gas atom is in the range of 2.5–4.5 Å,[28] we set the value of σ to be 3.56 Å according to the Lorentz–Berthelot mixing rules. The ϵ is chosen to be 0.05 eV and 0.5 eV, representing the case of weak and strong interaction between carbon and adatom, respectively. The reduced unit is used for the energy and the temperature, $E^{\star}=E/\epsilon$, $T^{\star}=k_BT/\epsilon$.

We bent[21] the graphite along the x and y axis in Fig. 1(a) to form zig–zag nanotubes [Fig. 1(c), $(n,0)$, with $n=9,10,...,18$] and armchair nanotubes [Fig. 1(b), (n,n), with $n=5,6,...,10$]. Periodic boundary conditions are imposed along the axial direction, with the length of a unit cell 25.56 and 24.60 Å, for zig–zag and armchair tube, respectively. There are 400 carbon atoms in the (10,10) calculating unit cell and 408 carbon atoms in the (17,0) one. Nanotubes with smaller diameter contain lesser number of carbon atoms in the unit cell. In the calculation of the graphite, we use a 240-atom unit cell with 12 atoms in the x axis and 20 atoms along the y axis. Periodic boundary conditions are imposed both along the x and y axis. All the C atoms in nanotubes and graphite are then relaxed by steepest descent method until the force on each of the atoms gets to zero.

On the basis of these obtained configurations, we studied the potential surface of the adatom on the nanotubes. Cylindrical coordinates (r,θ,z) is used to describe the location of the adatom in the nanotubes [Fig. 1(d)], where r denotes the distance of the adatom from the central axis of the nanotube, z is the coordinate along the central axis, θ is the polar angle. The curvature ρ of the surface is defined as the average curvature. For SWNTs it is the inversion of the diameter, i.e., $\rho=\sigma/D$, where D is the diameter of the tube. The sign of the curvature is defined so that ρ is positive for the exterior surface and negative for the interior surface of the nanotubes.

The energy surface $E(z,\theta)$ of the nanotubes and graphite was mapped out for the shaded area shown in Fig. 1 in the following way. The adatom is equidistantly placed at 100×100 positions (z,θ) on the inner and outer surface of the nanotube. Starting with the adatom at σ above the surface, at each (z,θ) position the total energy is minimized with respect to the r coordinate of the adatom, keeping all the carbon atoms fixed. Since the interaction between adatom and the carbon atoms are very weak comparing the interaction between carbon atoms, for simplicity, we fixed the coordinates of carbon atoms when we calculate the potential surface. As shown below, the dynamical simulation for the whole tube and adatom shows that the effect of the relaxation of carbon atoms is very small.

Microcanonical molecular dynamics simulations (MD) were performed on two typical armchair and zig–zag nanotubes, (10,10), (17,0), whose diameters are very close (13.56 Å and 13.31 Å). The adatom is put on the interior surface of the nanotube. All the freedoms of the carbon atoms and the adatom are let free, while keeping the center of the mass of the carbon nanotube fixed. The simulation temperature $T^{\star}$ for both of nanotubes are 0.001 for $\epsilon=0.05$ eV and 0.015 for $\epsilon=0.5$ eV. In all the simulations the time step is set to be 3.53 fs, with which the Newton's motion equations for atoms were integrated using the Verlet algorithm.[29] At each of the simulated temperatures, the trajectory of the adatom is followed for the 3.53 ns time interval.

III. RESULTS AND DISCUSSIONS

The diffusion paths are strongly curvature-dependent and helicity-dependent. What is shown in Fig. 2 is the potential energy surface, from which we can identify the diffusion paths. For the graphite plane, the diffusion path has a hexagonal symmetry, the diffusion along *ABA* and *ACA* has the same activation energy. The curvature of the nanotube breaks down the symmetry of those diffusion paths. For the positive curvatured armchair nanotube (exterior surface), the diffusion path *ABA* becomes more favorable than the *ACA* path, while the *ACA* path is more favorable for the positive curvatured zig–zag nanotube. However, on the negative curvatured surface, the *ACA* path is more favorable than *ABA* path for the armchair nanotube, and the *ABA* path is more favorable than the *ACA* path for the zig–zag nanotube.

To see this curvature effect in more detail, the curvature-dependent binding energies and diffusion barriers are given in Fig. 3, both for armchair and zig–zag SWNTs. The diffusion barrier is calculated as the difference between the lowest site and the saddle point along a certain path. We can see that the total energies of all the three sites increase with the surface curvature from negative to positive. Thus the binding of

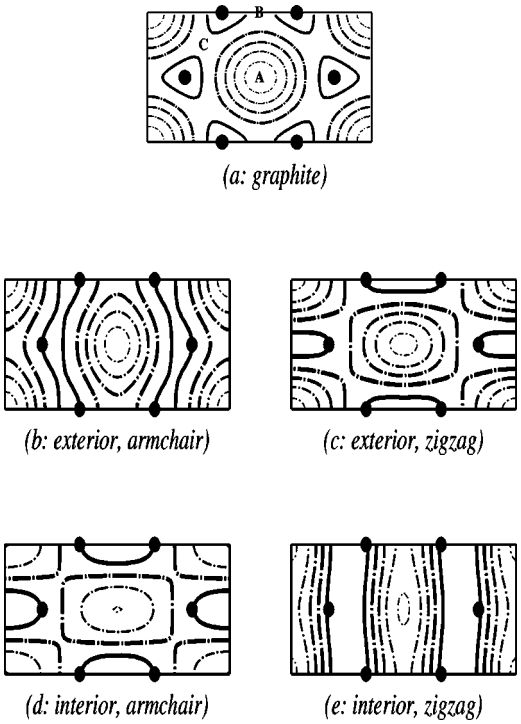

FIG. 2. The potential energy surface of the graphite sheet (a), and curvatured nanotubes; (b) positive curvatured armchair nanotube (exterior surface); (c) positive curvatured zig–zag nanotube (exterior surface); (d) negative curvatured armchair nanotube (interior surface); (e) negative curvatured zig–zag nanotube (interior surface). The thickness of the lines indicates the value of the height of the potential surface, and the solid line labels the highest value of the potential surface. It is suggested that nanotubes with different curvature and helicity can have quite different diffusion paths.

the adatom on the interior surface of the SWNTs is stronger than that on the graphite, while the binding on the graphite plane is stronger than that on the exterior surface. For both nanotubes with armchair and zig–zag helicity, the changes of the total energy of the binding site and the bridge sites are different, which leads to increasing diffusion barrier with

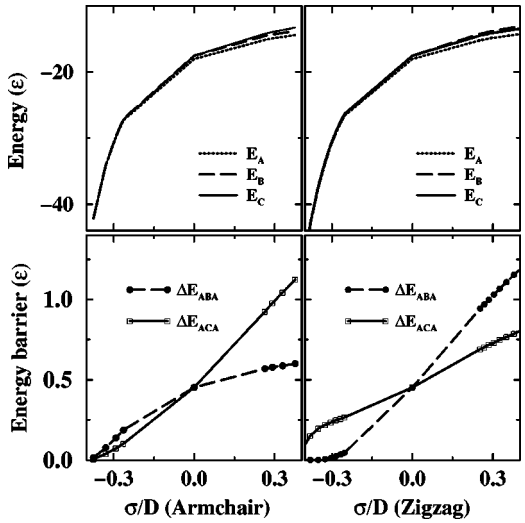

FIG. 3. (Upper panel) The binding energies for the *A*, *B*, and *C* sites, respectively, as a function of curvature. (Lower panel) The diffusion barrier for the two diffusion pathway *ABA* and *ACA*. The changes of the diffusion barriers with the curvature is quite different for different diffusion paths.

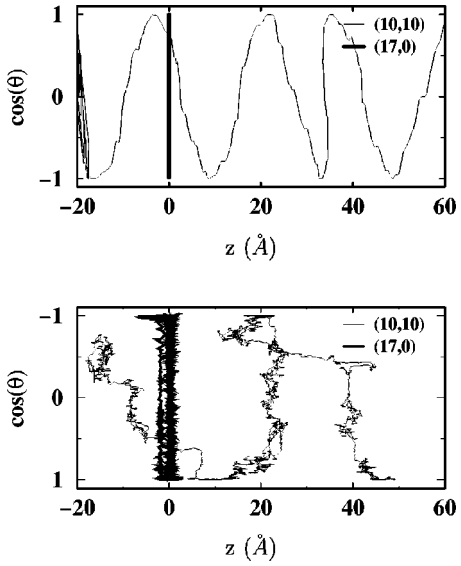

FIG. 4. The trajectories of an adatom diffusion in (10,10) and (17,0) nanotube. Upper panel is for $\epsilon = 0.05$ eV and $T^{\star} = 0.001$, and the lower panel is for $\epsilon = 0.5$ eV and $T^{\star} = 0.015$. The periodic changes of $\cos(\theta)$ with z indicates that the adatom diffuses helically along the z direction in the armchair nanotube, while the adatom in the zig–zag nanotube essentially circles around the axis, without displacement in the z direction. Evidently the axial diffusion of the adatom is much easier in the armchair nanotube than in the zig–zag one.

curvature. The lower panels of Fig. 3 show the change of the energy barrier with the surface curvature, from which one can easily see how the curvature changed the diffusion pathways. Since the energy barrier increases monotonically with the increase of the curvature, we can conclude that the adatom diffuses much easier inside the tube than on the graphite sheet, and more difficult on the exterior surface of SWNTs than on the graphite surface. The stronger adsorption and easier diffusion of adatom in the nanotube can be very important for understanding many physical properties of nanotube.[20,26,27,30]

It is interesting to note that, the favorable diffusion path *ABA* in the zig–zag tube is just perpendicular to the axial direction, thus the adatom can only move circlewise around the axis. For an adatom inside the zig–zag nanotube, it is difficult to diffuse either further into the nanotube along the axial direction, or out of the nanotube. This could play a crucial role for the mass transportation in the zig–zag nanotube.

Dynamical simulation does confirm that the axial diffusion in the armchair nanotube is much easier than that in the zig–zag nanotube. Figure 4 shows the trajectories of the adatom diffusing in the (10,10) and (17,0) nanotube. For clarity the trajectory is shown only for about 0.1 ns interval, since it just repeats itself in longer time. The simulation results show quite different processes of the adatom diffusion in armchair and zig–zag nanotubes, although both of them have almost the same diameter and curvature. In the armchair nanotube, the adatom diffuses helically along the axial direction with its coordinate θ varying periodically with z, which is consistent with the *ACA* path, except for the initial oscillatory motion, shown on the left part in the upper panel of Fig. 4. In the zig–zag nanotube, however, the adatom just rotates

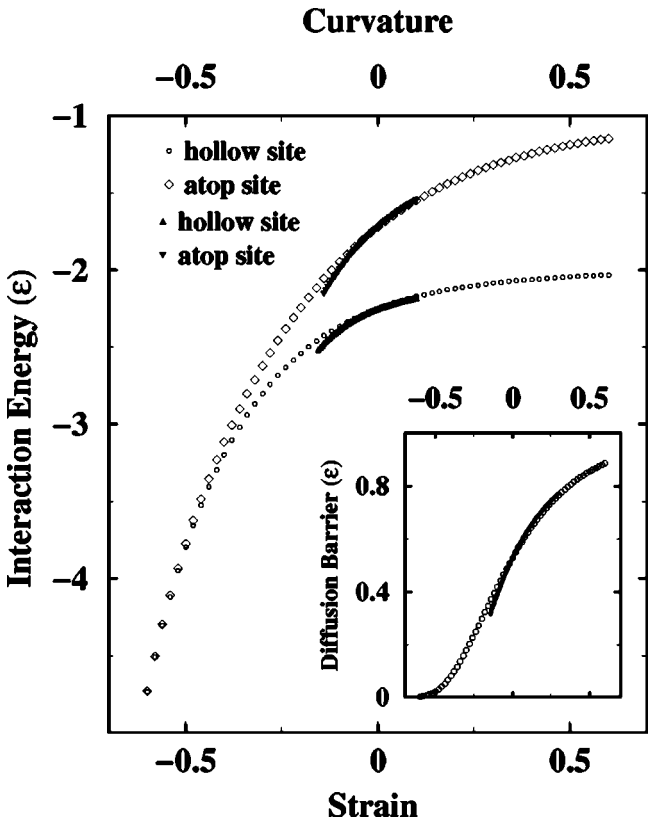

FIG. 5. The change of the potential energy and diffusion barrier (inset), the energy difference between the atop site and the hollow site, for an adatom over a simple modeled one dimension substrate. The open diamonds and open circles denote the potential energy and diffusion barrier with strain. The filled triangles and lines are for the changes with curvature. Within a certain range the strain and the curvature have the same effect on the adatom.

around the nanotube axis. With higher temperature and stronger interaction between carbon and adatom, the strong anisotropic diffusion process is still observed in the lower panel of Fig. 4, but significant fluctuations appear, which are caused by the thermodynamics and the relaxation of the C atoms.

One could understand how the curvature affects the adatom diffusion in terms of the tensile strain and the compressive strain. The effect of the strain on the adatom diffusion on the flat surface was reported before, mainly because of the practical application in the epitaxial growth.[8,31] It was found that the tensile strain makes the surface more corrugated and tends to raise the diffusion barrier, while the compressive strain smoothes the potential surface and decreases the diffusion barrier.[12,32] When the adatom is at the outer surface of a nanotube, the adatom *sees* a positive curvature surface which is similar to a tensile surface in a certain range, thus the diffusion barrier of the adatom is larger than that on a flat graphite plane. While the adatom is at the inner surface of a nanotube, the adatom *sees* a negative curvature surface which is similar to a compressive surface, the diffusion barrier of the adatom is decreased comparing to the nonstrained surface. However, it is worth to note that the curvature does not strain the surface homogeneously. So it is not a surprise that the curvature changes inhomogeneously the potential surface, and as a result, the most favorable diffusion path is changed.

In order to further compare the effect of the curvature and the strain, we used a simple one dimension model to see if the effect of the strain and the curvature on the diffusion properties have something in common. Interaction between the adatom and the one dimension substrate is described by the LJ potential. The substrate atoms are placed periodically with lattice parameter a. The diffusion barrier is calculated as the potential energy difference between the binding site and the bridge site. In the first model calculation, we keep all the substrate atoms in a straight line. The strain $(a-a_0)/a_0$ is switched by changing the lattice parameter a, where $a_0=\sigma$, σ is the LJ potential radius. In the second one, the lattice parameter is kept at a_0, but the one dimension substrate curved with a curvature $\rho=\sigma/D$, the sign of which is defined as above, D is the diameter of the curvature. Figure 5 shows the potential energy of the binding site and the bridge site, as a function of the strain and the curvature, respectively. Inset shows the corresponding diffusion barrier. We can see that the change of total energy in the two sites and thus the diffusion barrier are equivalent in the range $-0.1 \sim +0.1$ of the strain and the curvature. It suggests that the strain and the curvature do have similar effect on the potential energy and the diffusion barrier. Both the potential energy and the diffusion barrier increases, with the increasing of the curvature and the strain.

IV. SUMMARY

By calculating the potential energy surface and molecular dynamics with a model potential, we have carefully studied the diffusion of an adatom over nanotube surface. We found that, both the helicity and the curvature of the nanotube has important influence on the diffusion properties. Curvature, which can be considered as a kind of strain, changes the diffusion paths of the nanotube. Adatom diffuses along the axial direction more easily in armchair nanotubes than in zig–zag nanotubes. Positive curvature (exterior surface) raises the total energy and the diffusion barrier since it induces tensile strain. Negative curvature leads to compressive strain and smoothes the potential surface, therefore it lowers the diffusion barrier.

ACKNOWLEDGMENTS

This work is partially supported by NNSF of China, Pan-Den Project, CAS Project and the special funds for major state fundamental research project.

[1] F. Besenbacher, Rep. Prog. Phys. **59**, 1737 (1996).
[2] J. Nara, T. Sasaki, and T. Ohno, Phys. Rev. Lett. **79**, 4421 (1997).
[3] S. Jeong and A. Oshiyama, Phys. Rev. Lett. **79**, 4425 (1997).
[4] A. Sakai and T. Tatsumi, Appl. Phys. Lett. **64**, 52 (1994).
[5] H. Brune, M. Giovannini, and K. Bromann, Nature (London) **394**, 451 (1998).
[6] Q. Xie, A. Madhukar, P. Chen, and N. P. Kobayashi, Phys. Rev. Lett. **75**, 2542 (1995).
[7] C. S. Chang, Y. M. Huang, and T. T. Tsong, Phys. Rev. Lett. **77**, 2021 (1996).
[8] F. Liu, J. Tersoff, and M. G. Lagally, Phys. Rev. Lett. **80**, 1268 (1998).
[9] V. Holy, G. Springholz, M. Pinczolits, and G. Bauer, Phys. Rev. Lett. **83**, 356 (1999).

[10] P. Hanesch and E. Bertel, Phys. Rev. Lett. **79**, 1523 (1997).
[11] H. Brune, K. Bromann, H. Röder, K. Kern, J. Jacobisen, P. Stoltze, K. Jacobsen, and J. Nørskov, Phys. Rev. B **52**, R14380 (1995).
[12] C. Ratsch, A. P. Seitsonen, and M. Scheffler, Phys. Rev. B **55**, 6750 (1997).
[13] A. Bogicevic, J. Stromquist, and B. I. Lundqvist, Phys. Rev. Lett. **81**, 172 (1998).
[14] P. Kringhoj, A. N. Larseni, and S. Y. Shirayev, Phys. Rev. Lett. **76**, 3372 (1996).
[15] T. R. Mattsson, and H. Metiu, Appl. Phys. Lett. **75**, 926 (1999).
[16] J. Kärger and D. M. Ruthven, *Diffusion in Zeolites and Other Microporous Solids* (Wiley, New York, 1992).
[17] S. Iijima, Nature (London) **354**, 56 (1991).
[18] Q. Wang, S. R. Challa, D. S. Sholl, and J. K. Johnson, Phys. Rev. Lett. **82**, 956 (1999).
[19] T. W. Ebbesen, Annu. Rev. Mater. Sci. **24**, 235 (1994).
[20] A. C. Dillon, K. M. Jones, T. A. Bekkedahl, C. H. Kiang, D. S. Bethune, and M. J. Heben, Nature (London) **386**, 377 (1997).
[21] T. W. Odom, J.-L. Huang, P. Kim, and C. M. Lieber, Nature (London) **391**, 62 (1998).
[22] D. W. Brenner, Phys. Rev. B **42**, 9458 (1990).
[23] M. B. Nardelli, B. I. Yakobson, and J. Bernholc, Phys. Rev. Lett. **81**, 4656 (1998).
[24] S. E. Weber, S. Talapatra, C. Journet, A. Zambano, and A. D. Migone, Phys. Rev. B **61**, 13150 (2000).
[25] F. Darkrim and D. Levesque, J. Chem. Phys. **109**, 4981 (1998).
[26] G. Stan and M. W. Cole, Surf. Sci. **395**, 280 (1998).
[27] G. Stan and M. W. Cole, J. Low Temp. Phys. **101**, 539 (1998).
[28] G. Stan, M. J. Bojan, S. Curtarolo, S. M. Gatica, and M. W. Colo, Phys. Rev. B **62**, 2173 (2000).
[29] M. P. Allen and D. J. Tildesley, in *Computer Simulation of Liquids* (Oxford University Press, New York, 1987).
[30] K. G. Ayappa, Chem. Phys. Lett. **282**, 59 (1998).
[31] F. Liu, S. E. Davenport, H. M. Evans, and M. G. Lagally, Phys. Rev. Lett. **82**, 2528 (1999).
[32] B. D. Yu and M. Scheffler, Phys. Rev. B **56**, R15569 (1997).